Journal of The Electrochemical Society, **165** (11) C830-C834 (2018)
0013-4651/2018/165(11)/C830/5/$37.00 © The Electrochemical Society

The Effect of Short-Range Order on Passivation of Fe-Cr Alloys

Minglu Liu, Ashlee Aiello, Yusi Xie, and Karl Sieradzki [z]

Fulton School of Engineering, Arizona State University, Tempe, Arizona 85287-6106, USA

While it is well known that 12–13 at.% chromium is required for stainless-like passivation behavior of binary Fe-Cr alloys, there remain outstanding questions regarding the compositional dependence of this behavior. In order to explore these issues, we examined the passivation behavior of short-range ordered (SRO) Fe-Cr alloys and compared this to that of their random solid solution counterpart. Our results reveal that for alloys containing between 12–18 at.% Cr, passivation in the SRO alloys is delayed and we attribute this to ordering effects on percolation behavior. Finally, we discuss some major outstanding questions regarding passivation in the Fe-Cr system and suggest that first-principles based calculations could make important contributions to our understanding of passivation in this system.
 [DOI: 10.1149/2.0871811jes]

Manuscript submitted June 18, 2018; revised manuscript received August 17, 2018. Published August 30, 2018.

Austenitic stainless steels and binary Fe-Cr and Ni-Cr alloys are well known for their excellent corrosion behavior owing to the existence of a thin, ∼2 nm passive film, that has the ability to self-heal. That is, if a scratch breaches the film or if it is otherwise compromised, it reforms in aqueous environments. This self-healing behavior serves as a model for the development of modern corrosion protection coating schemes for other families of alloy systems including aluminum and magnesium.

A face centered cubic (fcc) austenitic stainless steel, such as 304 or 316 contains approximately 18 at.% Cr and 10 at.% Ni. However, one of the best-known facts in corrosion science is that only about 13 at.% (12 wt%) Cr is sufficient to prevent rusting in moist atmospheres or mildly acidic media.[1,2] The composition and structure of the passive film that forms in aqueous media on stainless steels has been extensively studied both in situ and ex situ over the past 50 years using the entire array of surface science spectroscopy techniques, electrochemical techniques, scanning probe and transmission electron microscopy.[3] Additionally, the breakdown of the passive film in aqueous media containing halides has also been extensively studied and modeled.[3] Nevertheless, we currently know very little about the initial stages of passivation, and also the latter stage processes during which the film adopts a crystalline structure.

In order to more clearly elucidate the issues associated with passivity in stainless steels we consider the behavior of the binary Fe-Cr system, which has been extensively studied. Figure 1 shows typical linear sweep voltammetry (LSV) behavior for Fe-Cr alloys in 0.5 M H_2SO_4.[4] Elemental Fe passivates at ∼+550 mV (SHE) whereas elemental Cr passivates at ∼−300 mV (SHE). These data are typical of those obtained in similar electrolytes by other investigators.[2,5] If one examines the passivation potential and the critical current density for passivation versus the Cr concentration a rather sharp decrease in these parameters occurs in the range of 10−14 at% Cr. Below this range in Cr concentration the alloy behavior is said to be "Fe-like" and above this range the behavior is "Cr like". The classical 13 at.% Cr threshold appears as a so-called reactivation potential, E_r[a]. That is, following the development of the passive film at high potentials, if one reverses the potential scan; dissolution is reactivated at a composition-dependent E_r owing to the reductive dissolution of Fe III oxide that forms at potentials more positive than E_r.

Although elemental Cr is more electrochemically active (less-noble equilibrium potential), owing to its ability to passivate at low potentials compared to Fe, it behaves as the more-noble component (i.e., it is kinetically stabilized) in the alloy while Fe is selectively dissolved.[6–8] Selective dissolution of Fe allows for the Cr surface concentration to increase eventually resulting in the evolution of a primary protective film. Since all the Cr concentrations in Figure 1 are below the three-dimensional (3D) Cr site percolation threshold, the immediate question that arises is what prevents existing Cr-oxide/hydroxide surface clusters and those that form during selective dissolution from being undercut?[9] If undercutting did not occur, we would expect that even for alloys dilute in Cr, Fe dissolution would result in the eventual evolution of a primary protective film. For example, consider the behavior of a Fe_pCr_{1-p} alloy in acid during the passivation process. Assuming selective dissolution of Fe occurs, the surface concentration of the Fe as a function of the number of equivalent monolayers dissolved, N, is simply given by p^N where p corresponds to the initial atom fraction of Fe in the alloy.[10] For a 5 at.% Cr alloy only 3 monolayers of dissolution would result in a surface concentration of Cr of ∼14 at.% for which one might expect to observe Cr-like passivation behavior. We know of course that a $Fe_{0.95}Cr_{0.05}$ alloy never displays this behavior and this taken together with Frankenthal's identification of the primary passivation process[11–13] was behind the conjecture developed by Sieradzki and Newman for the concentration dependence of passivation of Fe-Cr alloys.[14–16] At that time, they proposed that *long-range* percolation, i.e., involving 2nd and 3rd nearest neighbors (nn) could account for the concentration dependent passivation behavior. The neighbor distances in the bcc Fe-Cr lattice (1st nn $= a\sqrt{3}/2$; 2nd nn $= a$; 3rd nn $= a\sqrt{2}$, where a the lattice parameter $= 2.87$ Å) taken together with the hard sphere ionic radii for Cr^{3+} (0.69 Å) and O^{2-} (1.40 Å) set the appropriate long-range percolation length scale insuring the continuity of an incipient 3-dimensional Cr-O-Cr polymer-like network that was envisioned to represent the primary passivation structure and prevent undercutting. Based on the hard sphere ionic radii, the maximum Cr atom separation distance in a Cr-O-Cr mer-unit is 4.18 Å and this closely coincides with the 3rd nn distance of 4.06 Å. The percolation threshold for the bcc lattice including up to 2nd nn and 3rd nn, is 17.5% and 9.5% respectively.[17] Similar arguments were made for the fcc Ni-Cr system, for which they predicted that 13.6 at.% Cr was required for Cr-like passivation.

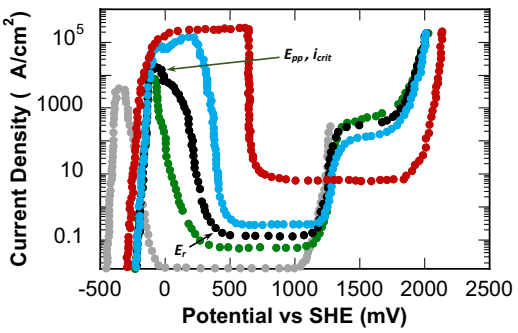

Figure 1. LSV behavior of Fe-Cr alloys. LSV behavior for elemental Cr (gray), elemental Fe (red), Fe-14 at.%Cr (green), Fe-10 at.%Cr (black), Fe-6 at%Cr (blue). Data adapted from Ref. 4. Indicated for the Fe-10 at.%Cr is the passivation potential, E_{pp} the "critical" current density for passivation, i_{pass} and the approximate location of the reactivation potential, E_r.

[z]E-mail: KARL.SIERADZKI@asu.edu

[a]In older literature, such as in the work of Uhlig[1,2] and Frankenthal,[10–12] E_r is sometimes referred to as the activation potential, E_a.

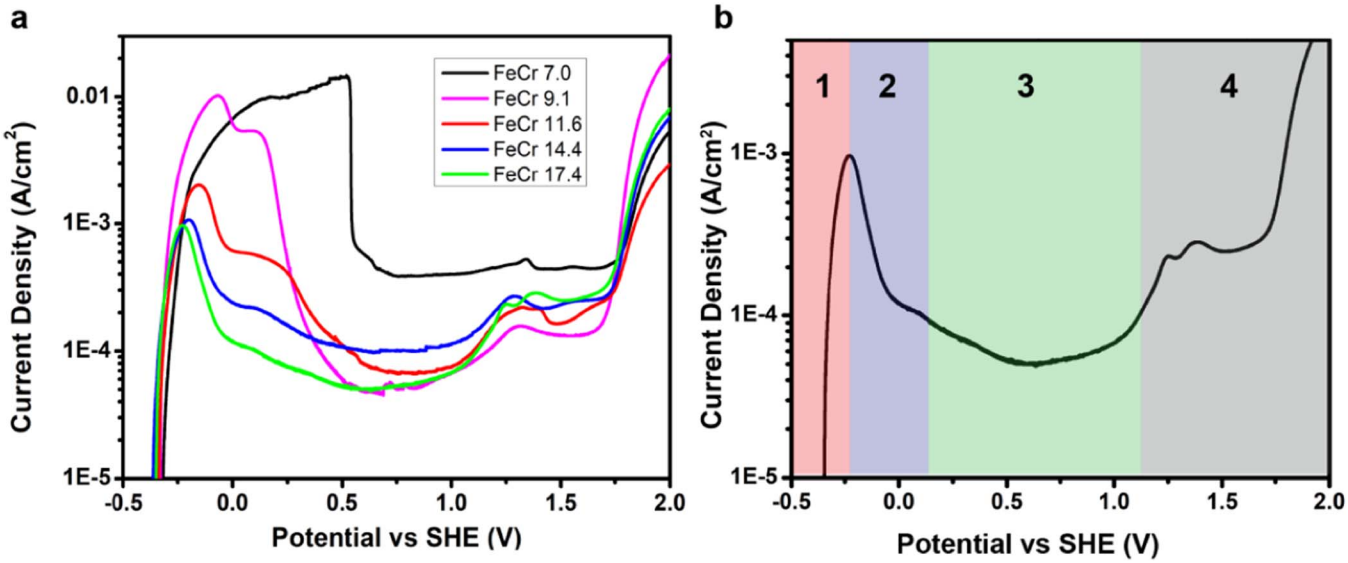

Figure 2. (a) Linear sweep voltammetry results of RSS Fe-Cr alloys with Cr concentration of 7.0 at.%, 9.1 at.%, 11.6 at.%, 14.4 at.% and 17.4 at.% (scan rate 10 mV/s). (b) Linear sweep voltammetry result on the RSS Fe-Cr 17.4% alloy defining four stages of the passivation process referred to in the text. 1. Active dissolution, 2. Primary passivation, 3. Passivation, 4. Trans-passive behavior.

In the compositional range of interest ∼ 5–20 at.% Cr, the conventional phase diagram for the binary Fe-Cr system is not well defined at temperatures below ∼800°C. Extrapolation of thermodynamic data predicts no solid-solubility of Cr in Fe at ambient temperature. Importantly, a growing number of first principles-based calculations show an inversion in the sign of enthalpy of mixing, H_{mix}, at ∼ 7–11 at% Cr.[18–24] Below this concentration, a single bcc phase is stable, H_{mix} is negative and the system has a tendency toward ordering. Above this composition, H_{mix} is positive (in the range of 0.01–0.02 eV/atom) and the system tends toward clustering of Cr-rich and Fe-rich, α + α' bcc phases. This inversion of H_{mix} is discussed in terms of magnetic frustration.[20] Elemental Fe is ferromagnetic (FM) and elemental Cr is antiferromagnetic (AFM). If a Cr atom (in a dilute Cr alloy) is placed in a Fe lattice the magnetic moment of Cr will be AFM aligned with respect to the Fe atom moments. As the Cr concentration in the alloy increases, random mixing statistics will result in the formation of Cr dimers, trimers, etc., within the Fe lattice. Several scenarios for the alignment of the Cr atom's magnetic moments are possible. If 2 nn Cr atoms align AFM with respect to each other, one of these moments will be FM aligned with respect to the surrounding Fe atoms. This high-energy configuration and other possible high energy configurations effectively enforce Cr-Cr atom repulsion at low concentrations and attraction at high concentrations (where H_{mix} changes sign). These first-principles based calculations predicting the inversion in H_{mix} have experimental verification from both neutron scattering[25] and Mössbauer spectroscopy studies.[26–28] The neutron scattering experiments examined the Cowley-Warren short-range order (SRO) parameter as a function of Cr composition in polycrystalline Fe_pCr_{1-p} alloys for $0 < 1\text{-}p < 0.15$. Samples were homogenized at 800°C and then heated in an evacuated quartz tube at 520°C to reach an equilibrium SRO state. Subsequently, the temperature was reduced to 430°C and maintained at this temperature for extended periods of time prior to a water quench. These results show an inversion in the SRO parameter occurs at 11.1 at.% Cr. The Mössbauer study examined Fe_pCr_{1-p} alloys for $0 < 1\text{-}p < 0.20$. Samples were heat treated in a manner similar to that described in the neutron scattering study. These results showed an inversion in the SRO parameter for the first and second neighbor shells occurring at ∼13 at.% Cr.

If the spatial separation between Cr atoms on a surface is an important aspect of the passivation process as conjectured by Sieradzki and Newman, SRO should alter the LSV behavior of properly heat-treated Fe-Cr alloys. Compared to that in a random solid-solution alloy, short-range order will reduce the average number of Cr atoms in the 1st nn shell of a "central" Cr atom. For example, consider the behavior of an alloy containing exactly 12.5 at.% Cr. For a random alloy this means on average that 1/8 of the nearest neighbors will be Cr, but for the short-ranged ordered alloy the average Cr population in the 1st shell will be reduced from this value. Consequently, the 3D site percolation threshold must increase to values larger than that of the random alloy and passivation of short-ranged ordered alloys should be delayed when compared to the behavior of a random alloy at the same composition. In order to test this, we performed LSV of Fe-Cr alloys (9.1 at% Cr, 11.6 at% Cr, 14.4 at% Cr and 17.4 at% Cr) that were subjected to heat treatments in order to obtain random and short-range ordered alloys.

Experimental

Master high-purity Fe-Cr alloys (99.85% Fe, 99.99% Cr, Goodfellow) were prepared by vacuum induction melting. The composition and homogeneity of all alloys was verified by energy dispersive spectroscopy (EDS). For electrochemical tests, electrodes were made into 5 mm diameter disks using electrical discharge machining. Prior to heat treatments, all samples were abraded to an 800-grit finish, and subsequently sealed in quartz tubes in an atmosphere of Ar for heat-treatment.

All heat treatments started with a homogenization step at 1100°C for 24 hours after which the temperature was lowered and maintained to 800°C for 24 hrs. A series of these samples (here termed random solid solution, "RSS") were water quenched from 800°C. In order to obtain short-ranged ordered, "SRO" samples, following the 800°C, 24 hour treatment, the temperature was lowered to 520°C for 24 hours (FeCr 17.4) or 430°C (FeCr 9.1, FeCr 11.6, FeCr 14.4) for 96 hours, following the protocols used in the neutron diffraction[25] and Mössbauer studies.[26–28] These samples were not abraded or polished prior to electrochemical testing following these heat treatments since such a procedure would destroy the SRO in the surface of the samples.

Linear sweep voltammetry (LSV) experiments were conducted in 0.1 M H_2SO_4 at scan rates of 10 mV/s and 1 mV/s using a Gamry series-G potentiostat. Platinum mesh was used as the counter electrode and a mercury-mercurous sulfate electrode (MSE) was used as the reference. All voltages in the manuscript are given with respect to the standard hydrogen electrode (SHE), where the conversion 0.00 V MSE = 0.64 V SHE was used. The electrolyte was de-aerated for

30 minutes using ultra high purity (UHP) nitrogen right before LSV runs. A two-step reduction protocol (−1.5 V vs MSE for 120 s and −1.2 V vs MSE for 30 s) was used to reduce the air-formed oxide on Fe-Cr surfaces. Hydrogen bubbles generated during oxide reduction were blown off from the surface by UHP nitrogen just prior to initiating LSV. During an experiment, nitrogen flow was maintained above the solution.

Results

Figure 2 shows LSV results for Fe-Cr alloys with random Cr distributions (RSS). As shown in Fig. 2a, among the five tested Fe-Cr alloys with random Cr atom distribution (7.0 at.%, 9.1 at.%, 11.6 at.%, 14.4 at.%, 17.4 at.%), the Fe-Cr 7.0 passivation behavior is distinct from the other four alloys. This alloy displays a broader dissolution plateau spanning 600 mV, which we believe occurs until most of the Fe in the alloy surface starts to passivate at ∼500 mV vs SHE. This type of behavior is similar to that of pure Fe, hence is categorized as "Fe-like". The Fe-Cr alloys with 9.1 at.%, 11.6 at.%, 14.4 at.% and 17.4 at.% Cr all exhibited "Cr-like" passivation behavior, where the dissolution peak is relatively sharp and occurs at a much lower potentials (below 0 V vs SHE). A general trend is that as the Cr concentration increases, both the passivation potential and the critical current density for Cr passivation decrease. The anodic polarization behavior of the RSS Fe-Cr alloys is in excellent agreement with many published reports.[2,4,5]

Four stages could be roughly identified in a typical "Cr-like" polarization curve, as shown in Figure 2b. The four stages represent active dissolution, primary passivation, passivation and trans-passive behavior, respectively. In the active dissolution stage Cr and Fe atoms are dissolved at different rates.[29,30] As the potential is increased, the alloy enters into the primary passivation regime, where continued selective dissolution of Fe occurs. The Cr surface concentration increases and Cr-O-Cr networks are forming. Owing to the length of the Cr-O bond, these networks can form among Cr surface atoms within 3rd near-neighbor distances.

Since Fe atoms separate Cr atoms at 2nd and 3rd neighbor distances, it seems likely that these Fe atoms are incorporated into the incipient passive film and are prevented from dissolving. This behavior is reflected in the abrupt current decay, and we refer this as primary passivation. At slightly higher potentials (composition-dependent), once percolating Cr-O-Cr networks exist, a significant fraction of the as yet non-passivated surface Fe is incorporated into an amorphous film forming a complicated network consisting of Fe-Cr oxide/hydroxide. Correspondingly, the dissolution current density continues to decrease and enters the passive regime. It should be noted that this "secondary" passivation behavior led by Fe participation is more clearly seen in Fe-Cr alloys in the range of ∼ 10–12 at.% Cr with the presence of a second dissolution wave (local maximum). In the present study, we focus on the primary passivation regime (region 2 of Fig. 2b), where Cr atomic ordering could affect the initial formation of Cr-O-Cr networks and subsequent Fe passivation behavior.

Figure 3 shows results of LSV experiments on the SRO and RSS alloys carried out at a scan rate of 1 mV/s (See Experimental Methods). Four sets of alloys (Fe-Cr 9.0, Fe-Cr 11.6, Fe-Cr 14.4 and Fe-Cr 17.4) were used to investigate the effect of SRO on the passivation behavior. We note that these results are representative of several experimental trials for both the RSS and SRO alloys for the compositions indicated. We first focus on the initial Cr-O-Cr network formation, "Cr passivation", defined by the first wave in Figs. 3b–3e. The largest difference between the RSS and SRO alloys is seen in the 11.6 at% Cr alloy (Fig. 3c). The passivation potential increased by more than 50 mV, and the corresponding critical current density for passivation in the SRO alloy is twice as large as the RSS alloy. Also, the Cr passivation in the RSS alloy results in a reduction of current density by one order of magnitude, whereas that of the SRO alloy decreased by less than 50%. These results indicate more rapid and efficient Cr passivation process in the RSS alloy compared to the behavior of the SRO alloy for the same Cr concentration. We believe that this difference in passivation behavior of the Fe-Cr at.% 11.6 alloy can be understood by considering the likely effect of SRO on percolation. Since, on average, SRO tends to increase the average separation between Cr nearest neighbor atoms in the alloy, we can expect that this would result in an increase in the percolation threshold and delayed passivation behavior. At lower Cr concentrations, e.g., 9.1 at.%, the average separation between Cr atoms is too low to allow for efficient network formation and correspondingly there is little difference in the first waves in Fig. 3b. Nevertheless, we observe a slightly deeper minimum for the RSS alloy following the first wave indicating more efficient formation of Cr-O-Cr networks that incorporate Fe. This is also observed in the behavior of the second wave that displays higher current densities for the SRO alloy. In the Fe-Cr 14.4 and Fe-Cr 17.4 at.% alloys, the Cr concentrations are 3–6 percent above the RSS percolation threshold, so it seems likely that percolation over 2nd and/or 3rd nearest neighbor Cr atoms also occurs for the SRO alloys at these compositions. Interestingly, the SRO 14.4 at.% Cr alloy shows a second wave while its RSS counterpart does not. This second wave must be related to Fe dissolution indicating some subtle differences in the way that Fe is incorporated into the primary passive film. Somewhat similar behavior is seen in the comparison of the 17.4 at.% alloy as the passive current density of the SRO alloy is larger than that in the RSS alloy.

Discussion

A key aspect of the current study was the previous neutron diffraction[25] and Mössbauer work[26–28] that provided us with protocols for obtaining short-range ordered alloys. At 800°C, Fe and Cr atoms are well mixed, hence quenching from this state yields random solid solution alloys.[31,32] Annealing at intermediate temperature allows for the redistribution of Cr atoms, and over a certain composition range the establishment of SRO in the alloy. We note that while the conventional Fe-Cr phase diagram shows that phase separation is thermodynamically favored at 400–500°C for Cr contents greater than ∼7–8 at.% Cr, this transformation is extremely sluggish.[31,32] Phase separation was experimentally observed in Fe-Cr containing Cr contents in the range of 20–35 at% (deep within the spinodal region of the phase diagram) upon thermal aging,[31,32] but the kinetics were quite slow. As a reference, in a 20 at.% Cr alloy annealed at 475°C for 50 hours, only 2% of the volume was transformed.[31] Hence, it seems safe to assume that for the alloy compositions and the annealing temperatures/times we used, phase separation was negligible.

It is important to point out that the different passivation behaviors we identified for the RSS and SRO alloys does not derive from a surface segregation process resulting from the heat treatments used. We note that some literature incorrectly attributes the passivation behavior of Fe-Cr alloys to a surface segregation process.[33] Clearly, this notion is inconsistent with the self-healing behavior of binary Fe-Cr alloys and stainless steels. Additionally, at scan rates of 1 mV/s, the peak current density in the active dissolution regime is of order 1 mA/cm^2 corresponding to the removal of ∼ 2–3 equivalent monolayers monolayer per second. In the case of the 11.6 at.% Cr alloy this corresponds to the removal of several hundred monolayers of alloy prior to the occurrence of the peak in the first dissolution wave.

We attribute the occurrence of the 2nd wave primarily to passivation of Fe atoms that are not located within Cr-O-Cr networks. While the mechanism of pure Fe passivation in sulfuric acid is still somewhat an open issue, it seems likely that it is a result of a salt film precipitation process and subsequent pH increases at the metal/salt film interface. The increase in pH allows for oxide formation, which can result in the eventual chemical dissolution of the salt film. Once the salt film dissolves, the oxide now exposed to the low pH electrolyte chemically dissolves and the Fe surface is once again activated to electrochemical dissolution. This scenario results in oscillatory behavior in the electrochemical current (or voltage under chronopotentiometry conditions). There are many observations of such oscillatory behavior for Fe in sulfuric acid.[34] Oscillatory behavior has also been seen in Fe-Cr alloys in pH 1–2 sulfate electrolytes containing up to 5 at.% Cr.[35] At higher Cr concentrations (e.g., 7.5at. %), two waves appear in the LSV and

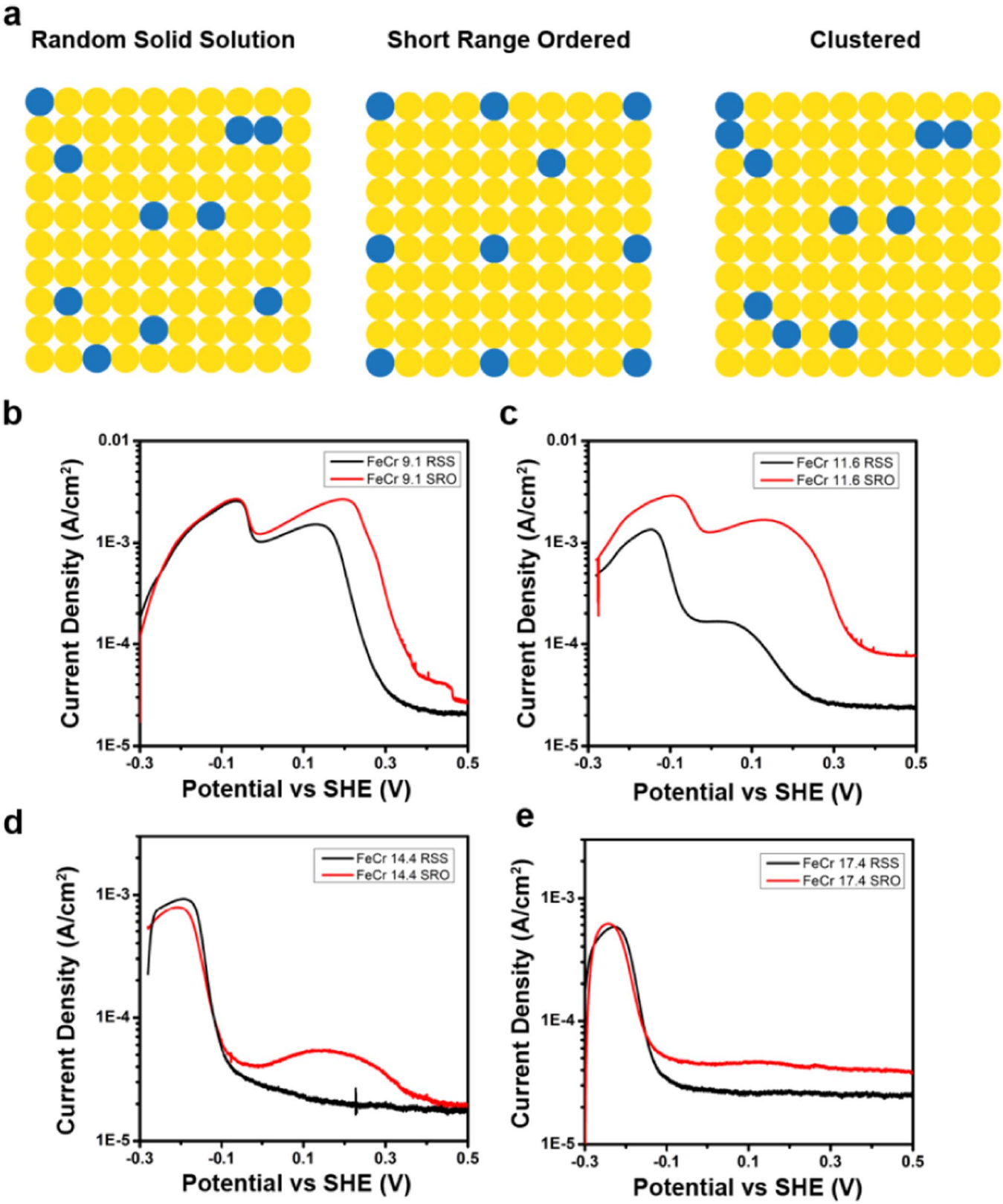

Figure 3. Comparison of LSV behavior for the RSS and SRO alloys. (a) Cartoons of 11.8% Fe-Cr alloy surface with random solid-solution, short-range ordered and clustered Cr distributions. LSV results on RSS (black-colored curves) and SRO (red-colored curves) alloys with different Cr concentrations at a scan rate of 1 mV/s. (b) 9.1 at.% Cr, (c) 11.6 at.% Cr, (d) 14.4 at.% Cr and (e) 17.4 at.% Cr. Sweep rate 1 mV/s.

the oscillatory behaviors are no longer present. This behavior is what has motivated us to suggest that the second wave in the LSV behavior is mainly associated with the passivation of Fe in the alloy.

There are several important questions that have to be resolved before we can hope to achieve a more complete understanding of the passivation behavior of Fe-Cr alloys. Electronic and Cr-Cr-cluster size effects connected to how Cr alloyed with Fe affects the dissociative adsorption of H_2O and OH^- and corresponding bonds energies of oxygen with Fe (and Cr) in the alloy is an outstanding question. For example, consider the behavior of a Fe-Cr alloy in the dilute Cr limit. What is the electrochemical potential at which a single Cr surface atom catalyzes the dissociative adsorption of H_2O or OH^-? How is the dissolution energy of the Cr atom affected by Fe? Consider this question for Cr clusters (dimers, trimers, etc.) of various size. Using a similar approach, we need to understand whether Cr atoms separated by 2nd and 3rd nn distances can dissociatively adsorb H_2O or OH^-. Many of these issues are simillar to questions that arise in catalysis on alloy surfaces and are often referred to as so-called geometric *ensemble size effects* and electronic structure-based *ligand effects*.[36] First principles-based calculations have made major contributions to our understanding of such issues in electrocatalysis (e.g., di-oxygen reduction on Pt and Pt alloys[36]) and it seems likely that such calculations could make a major contribution to our understanding of alloy passivation. In the case of Fe-Cr alloys such calculations would have to include magnetic effects. We hope that our brief discussion of these issues will motivate such calculations.

Conclusions

Our results show that Fe-Cr alloys in the range of ∼9–18 at.% Cr, heat treated to obtain short-range order, display delayed passivation behaviors compared to their random solid solution counterparts. These experiments have revealed the importance of nearest neighbor populations in affecting passivation behavior and therefore support the Sieradzki and Newman conjecture that such effects are vital to our understanding of passivation in this alloy system. Our results also highlight the necessity of first-principles based calculations for obtaining a better understanding passivation.

Acknowledgments

The authors gratefully acknowledge support of this work by the National Science Foundation under award DMR-1708459.

ORCID

Karl Sieradzki https://orcid.org/0000-0002-4789-3956

References

1. H. H. Uhlig and G. E. Woodside, "Anodic Polarization of Passive and Non-passive Chromium–Iron Alloys," *J. Phys. Chem.*, **57**, 280 (1953).
2. H. H. Uhlig and S. S. Lord, "Amount of Oxygen on The Surface of Passive Stainless Steel," *J. Electrochem. Soc.*, **100**, 216 (1953).
3. E. McCafferty, *Introduction to Corrosion Science*, Springer Publishing, New York, New York, (2010), ISBN 978–1441904546.
4. R. Kirchheim, B. Heine, H. Fischmeister, S. Hofmann, H. Knote, and U. Stoltz, "The Passivity of Iron-Chromium Alloys" *Corros. Sci.*, **29**, 899 (1989).
5. Y. A. Kolotyrkin, "Electrochemistry of Iron-Chrome-Nickel Alloys," in *Stress Corrosion Cracking and Hydrogen Embrittlement of Iron Base Alloys*, Edited by, R.W. Staehle, J. Hochmann, R.D. McCright, and J.E. Slater, National Association of Corrosion Engineers (NACE), Houston Texas, 946 (1977).
6. D. Hamm, K. Ogle, C.-O. Olsson, S. Weber, and D. Landolt, "Passivation of Fe–Cr Alloys Studied with ICP-AES and EQCM," *Corros. Sci.*, **44**, 1443 (2002).
7. J. E. Castle and J. H. Qiu, "A Co-Ordinated Study Of The Passivation Of Alloy Steels by Plasma Source Mass Spectrometry and X-Ray Photoelectron Spectroscopy—1. Characterization of The Passive Film," *Corros. Sci.*, **29**, 591 (1989).
8. A. J. Davenport, M. P. Ryan, M. C. Simmonds, P. Ernst, R. C. Newman, S. R. Sutton, and J. S. Colligon, "In Situ Synchrotron X-Ray Microprobe Studies of Passivation Thresholds in Fe-Cr Alloys," *J. Electrochem. Soc.*, **148**, B217 (2001).
9. R. C. Newman, F. T. Meng, and K. Sieradzki, "Validation of a Percolation Model for Passivation of Fe-Cr Alloys: I Current Efficiency In The Incompletely Passivated State," *Corros. Sci.*, **28**, 523 (1989).
10. K. Wagner, S. R. Brankovic, N. Dimitrov, and K. Sieradzki, "Dealloying Below The Critical Potential," *J. Electrochem. Soc.*, **144**, 3545 (1997).
11. R. P. Frankenthal, "On The Passivity Of Iron-Chromium Alloys I. Reversible Primary Passivation And Secondary Film Formation," *J. Electrochem. Soc.*, **114**, 542 (1967).
12. R. P. Frankenthal, "On the Passivity of Iron-Chromium Alloys II. The Activation Potential.," *J. Electrochem. Soc.*, **116**, 580 (1969).
13. R. P. Frankenthal, "On the Passivity of Iron-Chromium Alloys III. Effect of Potential," *J. Electrochem. Soc.*, **116**, 1646 (1969).
14. K. Sieradzki and R. C. Newman, "A. Percolation Model for Passivation in Stainless Steels," *J. Electrochem. Soc.*, **133**, 1979 (1986).
15. S. Qian, R. C. Newman, R. A. Cottis, and K. Sieradzki, "Validation of a Percolation Model for Passivation of Fe-Cr Alloys: Two-Dimensional Computer Simulations," *J. Electrochem. Soc.*, **137**, 435 (1990).
16. S. Qian, R. C. Newman, R. A. Cottis, and K. Sieradzki, "Computer Simulation of Alloy Passivation and Activation," *Corros. Sci.*, **31**, 621 (1990).
17. V. K. S. Shante and S. Kirkpatrick, "An Introduction to Percolation Theory," *Adv. Phys.*, **20**, 325 (1971).
18. P. Olsson, I. A. Abrikosov, and J. Wallenius, "Electronic Origin Of The Anomalous Stability of Fe-Rich Bcc Fe-Cr Alloys," *Phys. Rev. B.*, **73**, 104416 (2006).
19. P. A. Korzhavyi, A. V. Ruban, J. Odqvist, J.-O. Nilsson, and B. Johansson, "Electronic Structure and Effective Chemical and Magnetic Exchange Interactions in Bcc Fe-Cr Alloys," *Phys. Rev. B.*, **79**, 54202 (2009).
20. T. P. C. Klaver, R. Drautz, and M. W. Finnis, "Magnetism and Thermodynamics of Defect-Free Fe-Cr Alloys," *Phys. Rev. B.*, **74**, 94435 (2006).
21. A. Froideval, R. Iglesias, M Samaras, S. Schuppler, P. Nagel, D. Grolimund, M. Victoria, and W. Hoffelner, "Magnetic And Structural Properties of FeCr Alloys," *Phys. Rev. Lett.*, **99**, 237201 (2007).
22. G. Bonny, D. Terentyev, and L. Malerba, "On the α–α′ Miscibility Gap of Fe–Cr Alloys," *Scripta Mater.* **59**, 1193 (2008).
23. A. V. Ruban and V. I. Razumovskiy, "First-Principles Based Thermodynamic Model of Phase Equilibria In BCC Fe-Cr Alloys," *Phys. Rev. B.*, **86**, 174111 (2012).
24. M. Levesque, E. Martínez, C.-C. Fu, M. Nastar, and F. Soisson, "Simple Concentration-Dependent Pair Interaction Model for Large-Scale Simulations of Fe-Cr Alloys," *Phys. Rev. B.*, **84**, 184205 (2011).
25. I. Mirebeau and G. Parette, "Neutron Study of The Short Range Order Inversion in Fe_{1-x} Cr_x," *Phys. Rev. B.*, **82**, 104203 (2010).
26. S. M. Dubiel and J. Cieslak, "Short-Range Order in Iron-Rich Fe-Cr Alloys as Revealed by Mössbauer Spectroscopy," *Phys. Rev. B.*, **83**, 180202 (2011).
27. S. M. Dubiel and J. Cieślak, "Effect of Thermal Treatment on the Short-Range Order in Fe–Cr Alloys," *Mater. Lett.*, **107**, 86 (2013).
28. S. M. Dubiel, J. Cieślak, and J. Żukrowski, "Distribution of Cr Atoms in The Surface Zone of Fe-Rich Fe–Cr Alloys Quenched into Various Media: Mössbauer Spectroscopic Study," *Appl. Surf. Sci.*, **359**, 526 (2015).
29. J. E. Castle and J. H. Qiu, "The application of ICP-MS and XPS to studies of ion selectivity during passivation of stainless steels," *J. Electrochem. Soc.*, **137**, 2031 (1990).
30. D. Hamm, K. Ogle, C.-O. Olsson, S. Weber, and D. Landolt, "Passivation of Fe–Cr Alloys Studied with ICP-AES and EQCM," *Corros. Sci.*, **44**, 1443 (2002).
31. S. Novy, P. Pareige, and C. Pareige, "Atomic scale analysis and phase separation understanding in a thermally aged Fe–20 at.%Cr alloy," *J. of Nucl. Mater.*, **384**, 96 (2009).
32. X. Xu, J. Odqvist, M. H. Colliander, M. Thuvander, A. Steuwer, J. E. Westraadt, S. King, and P. Hedstrom, "Structural Characterization of Phase Separation in Fe-Cr: A Current Comparison of Experimental Methods," *Metall. Mater. Trans.*, **47A**, 5942 (2016).
33. W. T Geng, "Cr segregation at the Fe-Cr surface: A first-principles GGA investigation," *Phys. Rev. B*, **68**, 233402 (2003).
34. R. Liu, M. Zhang, Q. Meng, B. Yuan, Y. Zhu, L. Li, and C. Wang, "Oscillations of pH at the Fe|H_2SO_4 interface during anodic dissolution," *Electrochem,. Comm.*, **82**, 103 (2017).
35. M. S. El-Basiouny and S. Haruyama, "The Polarization Behavior of Fe-Cr alloys In Acidic Sulphate Solutions in the Active Region," *Corros. Sci.*, **17**, 405 (1977).
36. T. Bligaard and J. K. Nørskov, "Ligand Effects in Heterogeneous Catalysis and Electrochemistry," *Electrochim. Acta*, **52**, 5512 (2007).